Progress In Electromagnetics Research, PIER 66, 1–14, 2006

CIRCUIT MODELS FOR 2-DIMENSIONAL EM ABSORPTION BY BIOLOGICAL BODIES

E. M. A. Elkaramany and F. G. A. El-Hadeed

Engineering Mathematics and Physics Department
Cairo University
Giza 12211, Egypt

Abstract—In this paper, new circuit models are used to calculate the induced fields in biological media exposed to an incident plane wave in the two-dimensional cases. These models represent the induced fields in the medium using the lossy long transmission line model [1]. The voltages and currents in the circuit model simulate the electric and magnetic fields in the medium. The response of the medium to the incident wave is represented by equivalent conduction and polarization current sources in the medium. These currents are used as the excitation sources in the circuit model from which the required induced fields are obtained. An accurate absorbing impedance boundary condition for open boundaries is used which considerably reduces the matrix dimensions. The validity of these models is tested in the problem of absorption of E- and H-waves by biological multilayered cylinders. Results are compared with available analytical and numerical solutions.

1. INTRODUCTION

Consider the problem of plane polarized wave incident on an inhomogeneous biological body of arbitrary cross-section. The body is placed along the z-axis, in free space, as shown in Figure 1. The time dependence is taken to be $\exp(j\omega t)$ and there is no variation with respect to z-direction. Two cases are considered here, the case of incident polarized E-wave and that of the polarized H-wave.

In case of incident polarized E-wave (E_z^i, H_x^i), the incident electric field is given by, $E_z^i = e^{-jky}$, and from Maxwell's curl equations for the incident field, we get,

$$\partial_y(E_z^i) \quad = \quad -j\omega\mu_o(H_x^i) \tag{1}$$

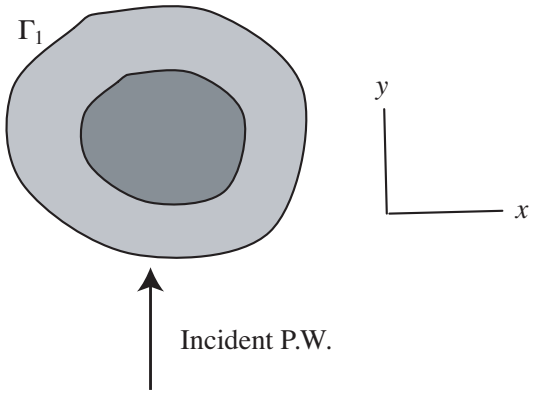

Figure 1. Problem of absorption of a plane wave by biological cylinder.

$$\partial_y(H_x^i) = j\omega\varepsilon_o(E_z^i) \tag{2}$$

while for the total fields (incident 'i' +induced 'd'), we have,

$$\partial_x(E_z^i + E_z^d) = j\omega\mu_o(H_y^d) \tag{3}$$

$$\partial_y(E_z^i + E_z^d) = -j\omega\mu_o(H_x^i + H_x^d) \tag{4}$$

$$\partial_x(H_y^d) - \partial_y(H_x^i + H_x^d) = j\omega\varepsilon^*(E_z^i + E_z^d) \tag{5}$$

where $\varepsilon^* = \left(\varepsilon - j\frac{\sigma}{\omega}\right)$, is the complex permittivity.

Substituting Equations (1) and (2) into Equations (3)–(5) we get,

$$\partial_x(E_z^d) = j\omega\mu_o(H_y^d) \tag{6}$$

$$\partial_y(E_z^d) = -j\omega\mu_o(H_x^d) \tag{7}$$

$$\partial_x H_y^d - \partial_y H_x^d = j\omega\varepsilon^* E_z^d + J_{ex} \tag{8}$$

where

$$J_{ex} = j\omega\varepsilon_o(\varepsilon_r^* - 1)E_z^i \tag{9}$$

Equations (6)–(8) show that the induced fields can be obtained by solving Maxwell's equations in the region of the medium which is exited by an excitation current density J_{ex}, representing the polarization and conduction current sources in the medium [2], and is given by Equation (9).

The set of Equations (6)–(8) can be written in the from,

$$\partial_x V_z = -ZI_x \tag{10}$$

$$\partial_y V_z = -ZI_y \tag{11}$$

$$\partial_x I_x + \partial_y I_y = -YV_z + J_{ex} \tag{12}$$

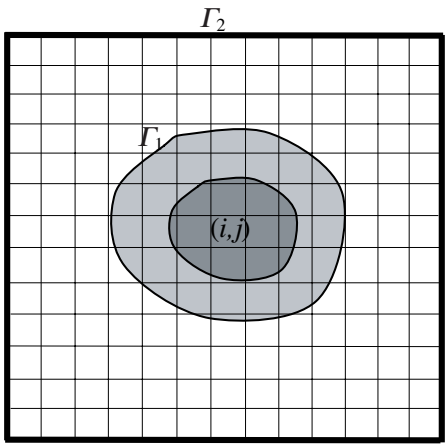

Figure 2. Region under study for the problem.

where

$$I_x \equiv -H_y^d, \qquad I_y \equiv H_x^d, \qquad V_z \equiv E_z^d \tag{13}$$

$$Z = j\omega\mu_o, \qquad Y \equiv j\omega\varepsilon^* \tag{14}$$

2. CIRCUIT MODEL AND ANALYSIS

Consider the region under study which contains the 2-dimensional biological body of complex permittivity $\varepsilon^*(x, y)$, which is bounded by an arbitrary boundary Γ_1.

To solve for the induced fields, the region is divided into N square cells of small dimensions $h \times h$ as shown in Figure 2. For a cell (i, j) in the medium, the symmetry of Equations (10)–(12) with respect to the two main directions x and y suggests the two cross-linked long transmission lines as shown in Figure 3 [3]. In this model, Equations (10) and (11) represent the relation between shunt voltages, while Equation (12) represents conservation of current at the cross nodes. The values of the characteristic impedance Z_c and the propagation constant γ are given by [1],

$$Z_c(i,j) = \sqrt{Z/Y} = R_c + jX_c = \sqrt{\frac{\mu_o}{\varepsilon^*(i,j)}} \tag{15}$$

$$\gamma(i,j) = \sqrt{ZY} = \alpha + j\beta = j\omega\sqrt{\mu_o\varepsilon^*(i,j)} \tag{16}$$

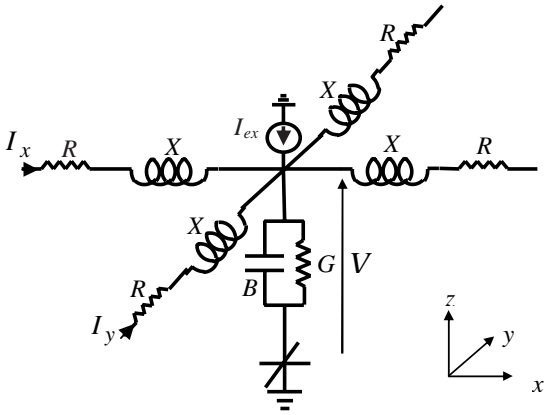

Figure 3. E-wave representation for node (i, j).

where

$$R_c = \sqrt{\frac{\mu_o}{\varepsilon_o}\frac{(1+\sqrt{1+T^2})}{2(1+T^2)}} \tag{17a}$$

$$X_c = \sqrt{\frac{\mu_o}{\varepsilon_o}\frac{(1-\sqrt{1+T^2})}{2(1+T^2)}} \tag{17b}$$

$$\alpha^2 = \frac{1}{2}\omega^2\mu_o\varepsilon_o\left(\sqrt{T^2+1}-1\right) \tag{17c}$$

$$\beta^2 = \frac{1}{2}\omega^2\mu_o\varepsilon_o\left(\sqrt{T^2+1}+1\right) \tag{17d}$$

and $T = \frac{\sigma}{\omega\varepsilon}$.

Using these values the long transmission line (LTL) series impedance $Z_s(i, j)$, and the parallel admittance $Y_p(i, j)$, are given by [1],

$$Z_s(i,j) = Z_c \tanh\left(\frac{\gamma(i,j)h}{2}\right) = R + jX \tag{18a}$$

$$Y_p(i,j) = \frac{2}{Z_c}\sinh\left(\gamma(i,j)h\right) = G + jB \tag{18b}$$

where

$$R = \frac{R_c\eta_1\left(1+\eta_2^2\right) - X_c\eta_2\left(1-\eta_1^2\right)}{1+(\eta_1\eta_2)^2} \tag{19a}$$

$$X = \frac{R_c\eta_2\left(1-\eta_1^2\right) + X_c\eta_1\left(1+\eta_2^2\right)}{1+(\eta_1\eta_2)^2} \tag{19b}$$

$$G = \frac{R_c \sinh(\alpha h)\cos(\beta h) + X_c \sin(\beta h)\cosh(\alpha h)}{R_c^2 + X_c^2} \quad (19c)$$

$$B = \frac{R_c \sin(\beta h)\cosh(\alpha h) - X_c \sinh(\alpha h)\cos(\beta h)}{R_c^2 + X_c^2} \quad (19d)$$

and $\eta_1 = \tanh\left(\frac{\alpha h}{2}\right)$, $\eta_2 = \tan\left(\frac{\beta h}{2}\right)$.

The node excitation current source $I_{ex}(i,j)$ represents the induced polarization and conduction currents and is given by,

$$I_{ex}(i,j) = Y_p(i,j)\left[\varepsilon_r^*(i,j) - 1\right] E_z^i(i,j) \quad (20)$$

The relation between the shunt voltage $V(i,j)$ at node (i,j) which is surrounded by the four cells $(i-1,j),(i+1,j),(i,j-1)$ and $(i,j+1)$, is given by,

$$\begin{aligned} &-Y_s(i,j-1)V(i,j-1) - Y_s(i-1,j)V(i-1,j) + Y_a(i,j)V(i,j) \\ &\quad -Y_s(i+1,j)V(i+1,j) - Y_s(i,j+1)V(i,j+1) = I_{ex}(i,j) \end{aligned} \quad (21)$$

where

$$Y_s(i,j-1) = \frac{1.0}{Z_s(i,j) + Z_s(i,j-1)} \quad (22)$$

is the admittance connected between the two adjacent nodes (i,j) and $(i,j-1)$. The values of $Y_s(i-1,j), Y_s(i+1,j)$, and $Y_s(i,j+1)$ are obtained in the same manner, while the value of admittance $Y_a(i,i)$ is given by,

$$Y_a(i,i) = Y_s(i,j-1)+Y_s(i-1,j)+Y_s(i+1,j)+Y_s(i,j+1)+Y_p(i,i) \quad (23)$$

which represents the sum of all admittances connected to the node (i,j).

For the free space outside the medium, $\alpha = 0$, $\beta_0 = \omega\sqrt{\mu_o \varepsilon_o}$ and $I_{ex} = 0$, so that Equation (21) can by written as,

$$-V(i,j-1) - V(i-1,j) + (4.0-\xi)V(i,j) - V(i+1,j) - V(i,j+1) = 0 \quad (24)$$

where

$$\xi = \frac{-Y_p}{Y_s} = 8\sin^2\left(\frac{\gamma h}{2}\right) \quad (25)$$

Equations for cells at boundaries Γ_1 and Γ_2 can be obtained easily in the same manner.

For the case of incident plane polarized H-wave (H_z^i, E_x^i), we have $H_z^i = e^{-jky}$, and the equations governing the induced fields in the

medium can be derived in same manner and are given by,

$$-\partial_x(H_z^d) = j\omega\varepsilon^* E_y^d \tag{26}$$

$$\partial_y(H_z^d) = j\omega\varepsilon^*(E_x^d) + j\omega\varepsilon^* \frac{(\varepsilon_r^* - 1)}{\varepsilon_r^*} E_x^i \tag{27}$$

$$\partial_x E_y^d - \partial_y E_x^d = -j\omega\mu_o H_z^d \tag{28}$$

These equations can be written in the form,

$$\partial_x(I_z) = -YV_y \tag{29}$$

$$\partial_y(I_z) = -Y(V_x) + I_{ex} \tag{30}$$

$$\partial_x V_y + \partial_y V_x = -ZI_z \tag{31}$$

where

$$V_x \equiv -E_x^d, \qquad V_y \equiv E_y^d, \qquad I_z \equiv H_z^d \tag{32}$$

Equations (29)–(31) suggest the two crossed ∂-form circuit model [4] shown in Figure 4.

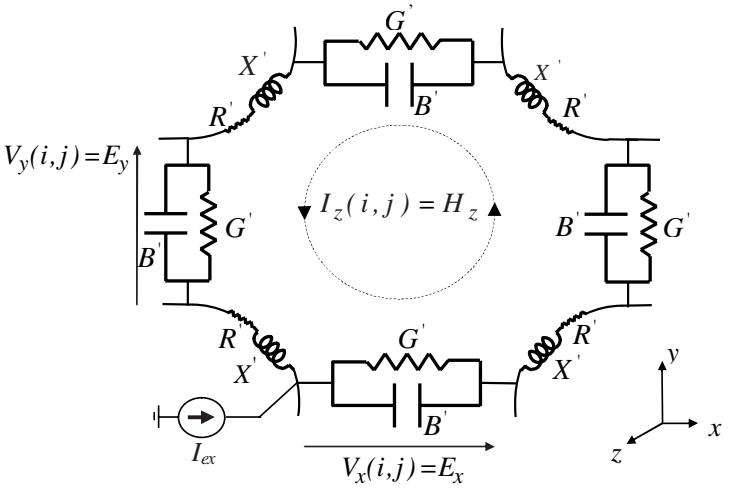

Figure 4. H-wave circuit model representation.

The characteristic impedance and the propagation constant are given as before in Equations (15)–(17), and in this case the series impedance $Z_s' = 4(R' + jX')$ and the parallel admittance $Y_p' = G' + jB'$ are given by,

$$Z_s' = Z_c \sinh(\gamma h) \tag{33}$$

$$Y_p' = \frac{1}{Z_c} \tanh\left(\frac{\gamma h}{2}\right) \tag{34}$$

and

$$R' = \frac{1}{4}\left[R_c \sinh(\alpha h)\cos(\beta h) - X_c \sin(\beta h)\cosh(\alpha h)\right] \quad (35)$$

$$X' = \frac{1}{4}\left[R_c \sin(\beta h)\cosh(\alpha h) + X_c \sinh(\alpha h)\cos(\beta h)\right] \quad (36)$$

$$G' = \frac{R_c\eta_1(1+\eta_2^2) + X_c\eta_2(1-\eta_1^2)}{(R_c^2+X_c^2)\,(1+(\eta_1\eta_2)^2)} \quad (37)$$

$$B' = \frac{R_c\eta_2(1-\eta_1^2) - X_c\eta_1(1+\eta_2^2)}{(R_c^2+X_c^2)\,(1+(\eta_1\eta_2)^2)} \quad (38)$$

In this case, equation of the loop current $I_z(i,j)$ for mesh representing node (i,j) is given by,

$$\begin{aligned} &-I_z(i,j-1)Z_x(i,j) - I_z(i-1,j)Z_y(i,j) - I_z(i+1,j)Z_y(i+1,j) \\ &-I_z(i,j+1)Z_x(i,j+1) + [Z'_s + Z_x(i,j) + Z_y(i,j) + Z_x(i,j+1) \\ &+Z_y(i+1,j)]\, I_z(i,j) = V_{ex}(i,j) \end{aligned} \quad (39)$$

where

$$V_{ex}(i,j) = \left[\frac{\varepsilon_r^*(i,j)-1}{\varepsilon_r^*(i,j)}\right] E_x^i(i,j) \quad (40)$$

and

$$Z_x(i,j+1) = \frac{1.0}{Y'_p(i,j) + Y'_p(i,j+1)} \quad (41)$$

is the impedance connected between the two adjacent meshes (i,j) and $(i,j+1)$. The values of all impedances Z_x and Z_y are obtained in the same manner.

Note that in the circuit, the excitation voltage source V_{ex} is replaced by an equivalent current source I_{ex}, given by,

$$I_{ex}(i,j) = Y'_p(i,j)\left[\frac{\varepsilon_r^*(i,j)-1}{\varepsilon_r^*(i,j)}\right] E_x^i(i,j) \quad (42)$$

For the free space outside the medium, the values of Z'_s and Y'_p are the same for all meshes, and Equation (39) can by written as,

$$[-I_z(i,j-1) - I_z(i-1,j) - I_z(i+1,j) - I_z(i,j+1)] + [4.0-\xi]\, I_z(i,j) = 0 \quad (43)$$

The N equations relating the node voltages in case of the incident polarized E-wave or the loop currents in case of the incident polarized H-wave can be arranged in the matrix form

$$[A]\ \ [B] = [C] \quad (44)$$

where $[A]$ is a banded matrix (with five diagonal vectors), which represent the admittance matrix ,in case of incident E-wave, or the impedance matrix, in case of incident H-wave. $[C]$ is the excitation vector. $[B]$ is the required induced field in each case.

The last system of equations is solved to get the unknown induced field. The total field at any point can be found by superposition of the incident and the induced fields at that point.

3. BOUNDARY CONDITIONS

Different boundary conditions which are used in the previous two-dimensional models are described in many papers [5, 6]. Symmetry plane is represented by a magnetic wall at which tangential component of the magnetic field vanishes, so, an open circuited boundary, can describe effectively the plane of symmetry and only one part of the two symmetric parts of the problem need to be modeled.

Open boundary can be terminated by the absorbing impedances [6] given by,

$$Z_{ter,x} = -\frac{E_z}{H_y} = -\frac{E_z}{H_\phi \cos\phi} = \frac{Z_{ter}}{\cos\phi} \tag{45}$$

at a plane $x = x_o$ and,

$$Z_{ter,y} = \frac{E_z}{H_x} = -\frac{E_z}{H_\phi \sin\phi} = \frac{Z_{ter}}{\sin\phi} \tag{46}$$

at a plane $y = y_o$, where, ϕ is the angle of incidence, and

$$Z_{ter,x} = Z_{ter,y} \approx Z_c \tag{47}$$

where $Z_c = \sqrt{\frac{\mu_o}{\varepsilon_o}}$ is the characteristic impedance of vacuum.

For E-wave, an accurate boundary impedance termination is given by [7],

$$Z_{ter} = jZ_c \frac{\mathbf{H}_o^2(kr)}{\mathbf{H}_o^{2\prime}(kr)} \tag{48}$$

where $\mathbf{H}_o^2$ is the second Hankel function of order 0. This absorbing boundary is proved to give accurate results at smaller distance ($kd \approx 1.0$) between the medium and the outer terminating boundary.

Note that when the termination boundary is at sufficient large distance from the body, asymptotic forms of Hankel function and its derivative lead to $Z_{ter} \approx Z_c$.

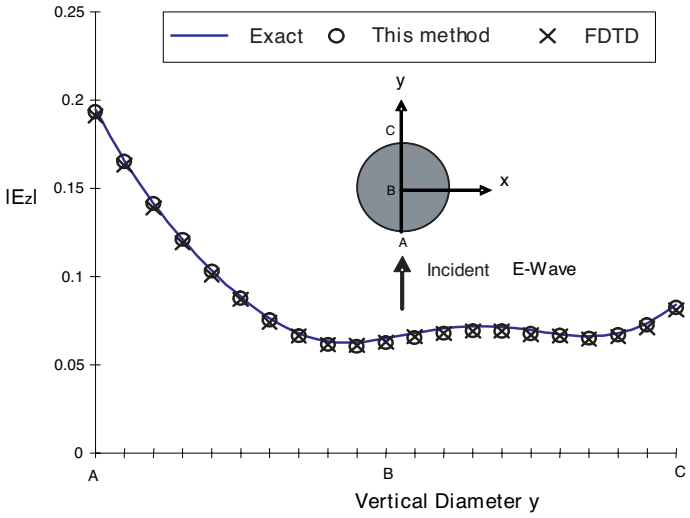

Figure 5a. Total electric field $|E_z|$ along y-axis for homogeneous muscle cylinder of radius 15 cm, $\varepsilon_r = 72, \sigma = 0.9\,\mathrm{S/m}$, illuminated by E-wave, 100 MHz.

4. RESULTS AND COMMENTS

To test the validity of the model, consider the case of two layered cylinder with an inner layer of radius 7.85 cm, and an outer layer of radius 15 cm. A grid of 21×21 squares is used to model this body.

Figure 5a shows the total electric field E_z along the vertical diameter of a homogeneous muscle cylinder ($\varepsilon_{r1} = \varepsilon_{r2} = 72$, $\sigma_1 = \sigma_2 = 0.9\,\mathrm{S/m}$), exposed to E-wave at 100 MHz. These results are compared with the exact series solution [2] and FD-TD method [8]. Figure 5b shows the obtained values of the total field along the horizontal axis for the same body.

Figures 6a and 6b show the results for a fat-muscle cylinder with an inner layer of muscle ($\varepsilon_{r1} = 72, \sigma_1 = 0.9\,\mathrm{S/m}$) and an outer layer of fat ($\varepsilon_{r2} = 7.5, \sigma_2 = 0.048\,\mathrm{S/m}$), exposed to E-wave at 100 MHz. Results are compared with the FD-TD method [8] and the exact solution [9].

Figures 7a, 7b and 7c show the results for the same fat-muscle cylinder but exposed to 100 MHz H-wave.

In the last examples, three sources of error in the model exist; the first is the staircase approximation for the curved surface of the cylinder, the second is the approximation of the absorption boundary conditions, which is greatly minimized when using the described

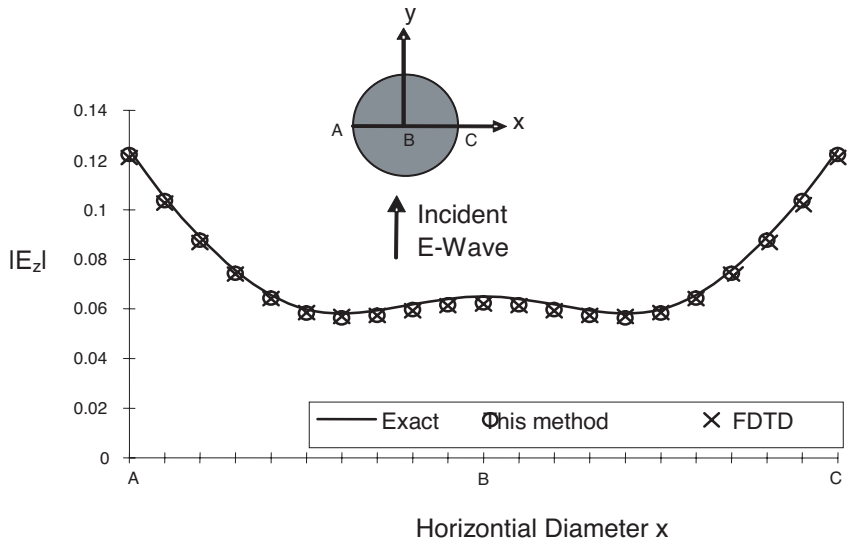

Figure 5b. Total electric field $|E_z|$ along x-axis for homogeneous muscle cylinder of radius 15 cm, $\varepsilon_r = 72$, $\sigma = 0.9\,\mathrm{S/m}$, illuminated by E-wave, 100 MHz.

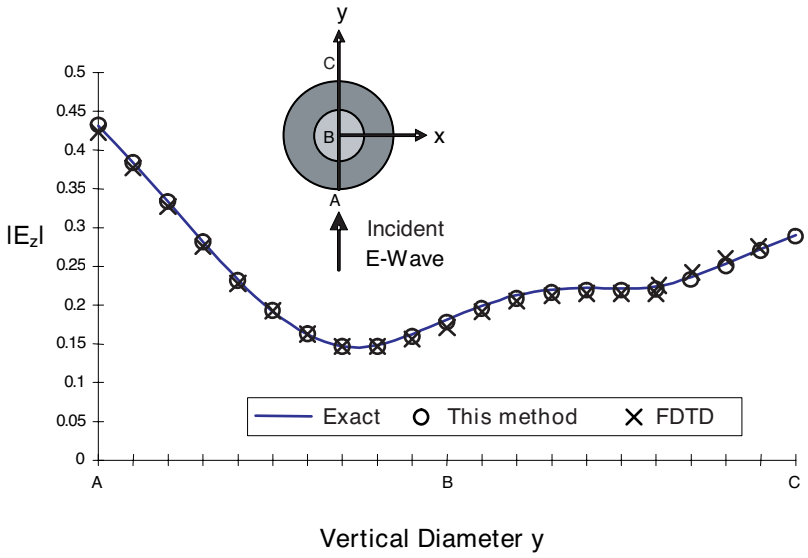

Figure 6a. Total electric field $|E_z|$ along y-axis for muscle-fat cylinder of radii 7.85 cm and 15 cm, $\varepsilon_{r1} = 72$, $\varepsilon_{r2} = 7.5$, $\sigma_1 = 0.9\,\mathrm{S/m}$, $\sigma_2 = 0.048\,\mathrm{S/m}$ illuminated by E-wave, 100 MHz.

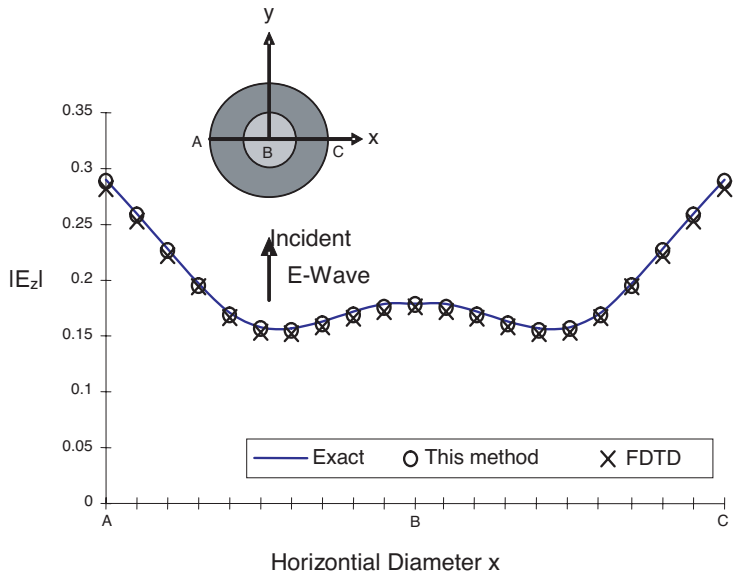

Figure 6b. Total electric field $|E_z|$ along x-axis for muscle-fat cylinder of radii 7.85 cm and 15 cm, $\varepsilon_{r1} = 72$, $\varepsilon_{r2} = 7.5$, $\sigma_1 = 0.9\,\mathrm{S/m}$, $\sigma_2 = 0.048\,\mathrm{S/m}$ illuminated by E-wave, 100 MHz.

absorbing boundary at Γ_2. The last is the approximation made in the values of the propagation constant in different directions. In two-dimensional model the propagation constants in the two directions of the transverse plane are locally equal, where the propagation constant in the network is approximated by $k = \sqrt{2}k_x = \sqrt{2}k_y$ [3], so, if the actual direction of propagation is in the diagonal direction of the model, the velocity of the wave in the model will coincide with the actual velocity in the medium. But in case of axial propagation, where the wave actually propagates in one of the network directions, the error depends on the ratio (h/λ) and the ratio of the velocity of waves in the network to the actual medium velocity $(v_n/v = \omega/k_n v)$ can be estimated from the relation [10],

$$\sin\left(\frac{k_n h}{2}\right) = \sqrt{2}\sin\left(\frac{\omega h}{2v}\right) \tag{49}$$

which shows that, the ratio (v_n/v) varies from $(1/\sqrt{2})$ at $h/\lambda = 0$ to 0.5 at $h/\lambda = 0.25$, and the model has a pass-bands filter characteristics where no propagation can occur in the network for frequencies over $(h/\lambda) = 0.25$.

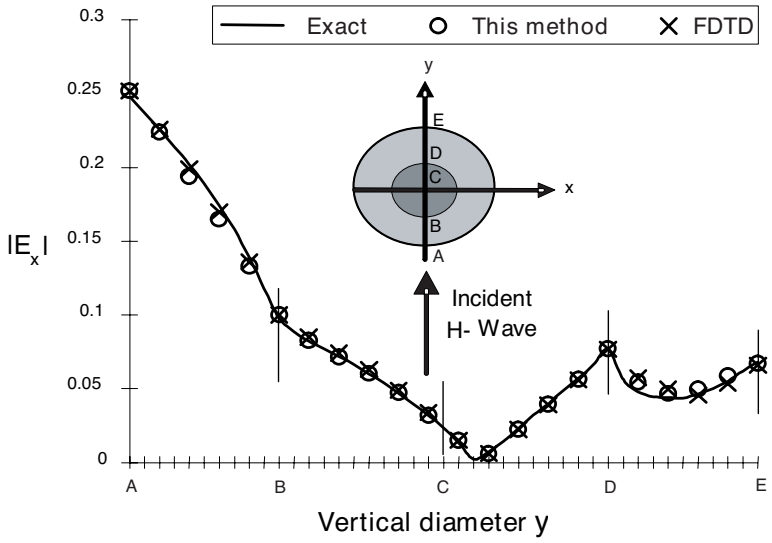

Figure 7a. Total electric field $|E_x|$ along y-axis for muscle-fat cylinder of radii 7.85 cm and 15 cm, $\varepsilon_{r1} = 72$, $\varepsilon_{r2} = 7.5$, $\sigma_1 = 0.9\,\mathrm{S/m}$, $\sigma_2 = 0.048\,\mathrm{S/m}$ illuminated by H-wave, 100 MHz.

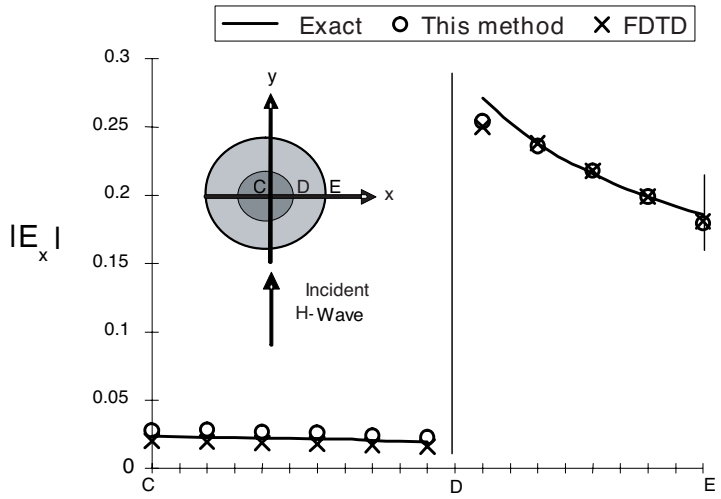

Figure 7b. Total electric field $|E_x|$ along x-axis for muscle-fat cylinder of radii 7.85 cm and 15 cm, $\varepsilon_{r1} = 72$, $\varepsilon_{r2} = 7.5$, $\sigma_1 = 0.9\,\mathrm{S/m}$, $\sigma_2 = 0.048\,\mathrm{S/m}$ illuminated by H-wave, 100 MHz.

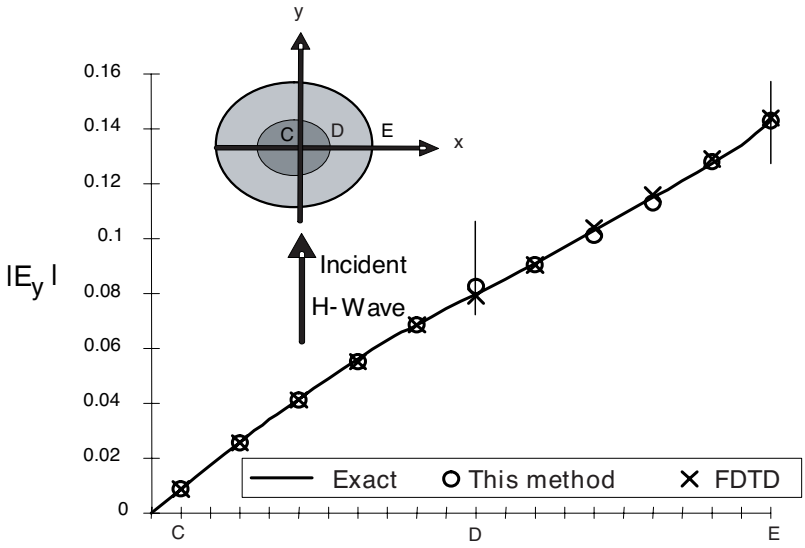

Figure 7c. Total electric field $|E_y|$ along x-axis for muscle-fat cylinder of radii 7.85 cm and 15 cm, $\varepsilon_{r1} = 72$, $\varepsilon_{r2} = 7.5$, $\sigma_1 = 0.9\,\mathrm{S/m}$, $\sigma_2 = 0.048\,\mathrm{S/m}$ illuminated by H-wave, 100 MHz.

5. CONCLUSION

In this work, the two-dimensional absorption problem is simulated using circuit models. The main advantages of these models are the simple representation of boundary conditions, the accurate results with smaller matrix size and the simple sparse matrix which can be easily derived and solved.

In most approximate methods, the effect of the absorbing boundary is shown in the rear region of the medium, where reflection from the approximate absorbing boundary greatly affects its magnitude. In this work, the results show that this effect is greatly minimized when using the impedance condition in Equation (48) for the case of E-wave at distance of the order of ($kd \sim 1.0$) from the medium boundary. This means that accurate results are obtained using reduced matrix size and computation time.

REFERENCES

1. Johnson, W. C., *Transmission Lines and Network,* 117–122, McGraw-Hill, New York, 1950.
2. Harrington, R. F., *Time Harmonic Electromagnetic Fields,* 362, McGraw-Hill, 1961.
3. Mohsen, A. A., M. H. S. Elmarkaby, and E. M. A. Elkaramany, "Two dimensional long transmission line-frequency domain (LTL-FD) treatment of waveguides," *Journal of Electromagnetic Waves and Application,* Vol. 14, 1399–1414, 2000.
4. Mohsen, A. A., E. M. A. Elkaramany, and F. G. Abo El-Hadeed, "Analysis of microwave cavities using LTL-FD method," *Journal of Electromagnetic Waves and Application,* Vol. 19, 145–162, 2005.
5. Zhizhang, C., M. M. Ney, and W. J. R. Hoefer, "A new boundary description in two dimensional TLM models of microwave circuits," *IEEE Trans.,* Vol. MTT-39, 377–382, 1991.
6. Simons, N. R. S., A. A, Sebak, and E. Bridges, "Transmission-line matrix method for scattering problems," *Computer Physics Communications,* Vol. 69, 197–212, 1991.
7. El-karamany, E. M. A., "New impedance boundary condition in two dimensional LTL-FD treatment of scattering problems," *Journal of Electromagnetic Waves and Application,* Vol. 17, 1269–1287, 2003.
8. David, T., M. Dennis, and P. Om, "Comparison of the FFT conjugate gradient method and the finite-difference time-domain method for the 2-D absorption problem," *IEEE Trans.,* Vol. MTT-35, 383–395, 1987.
9. Bussey, H. E. and J. H. Richmond, "Scattering by a lossy dielectric cylindrical multilayer, numerical values," *IEEE Trans. AP,* Vol. 23, 723–725, 1975.
10. Jhons, B. B. and R. L. Beurle, "Numerical solution of 2-dimensional scattering problems using a transmission line matrix," *Proc. IEEE,* Vol. 118, 1203–1208, 1971.